ACS Macro Letters

Letter

pubs.acs.org/macroletters

Achieving Diameter-Selective Separation of Single-Walled Carbon Nanotubes by Using Polymer Conformation-Confined Helical Cavity

Yusheng Chen,[†] Yongqian Xu,[†] Kelly Perry,[‡] Alexei P. Sokolov,[‡] Karren More,[‡] and Yi Pang*,[†]

[†]Department of Chemistry & Maurice Morton Institute of Polymer Science, University of Akron, Ohio 44325, United States

[‡]Oak Ridge National Laboratory, Oak Ridge, Tennessee 37831-6197, United States

Supporting Information

ABSTRACT: A water-soluble poly[(*m*-phenylenevinylene)-*alt*-(*p*-phenylenevinylene)] (PmPV) **2** has been synthesized, which exhibits an unsymmetrical substitution pattern on the *para*-phenylene unit. With one substituent being hydrophilic while the other being hydrophobic, the polymer chain has a higher tendency to fold in aqueous solution, thereby promoting helical conformation. The polymer is found to selectively disperse the single-walled nanotubes (SWNTs) of small diameters (d = 0.75−0.84 nm), in sharp contrast to PmPV **1** with a symmetrical substitution pattern. The intriguing diameter-based selectivity is believed to be associated with the confined helical conformation, which provides a suitable cavity to host the SWNT of proper sizes. The study thus provides a useful demonstration that the polymer conformation can have a profound impact on the SWNT sorting.

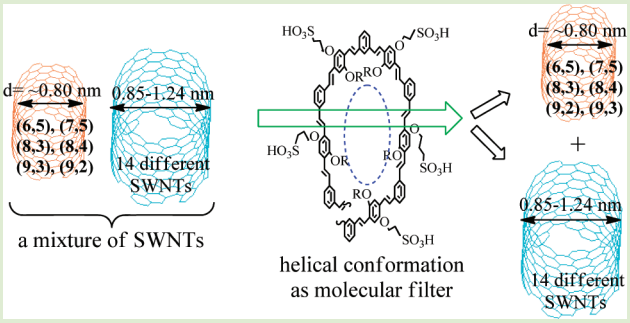

Single-walled nanotubes (SWNTs) exhibit superior mechanical,[1] electrical,[2,3] and electronic properties, which have demonstrated their unique advantages in various applications, including flexible electronics,[4] biosensors,[5] and transistors.[6] The electronic structure and optical properties of individual SWNTs are uniquely dependent on the chiral indices (n,m) which determine the tube's diameters.[7] The as-prepared sample, however, is generally a mixture of different SWNTs, including metallic and semiconducting ones.[8] Selective enrichment and effective isolation of individual chiral nanotube are essential to understand the fundamental physical properties of each SWNT species, which plays a vital role in the realization of the true application potential of SWNTs.

The separation of a specific tube from a mixture of SWNTs remains a major challenge, due to their structural similarity between the different SWNT species.[9] The chirality of SWNTs can be enriched from a mixture by using proper dispersing reagents, which include pyrene,[10] flavin,[11] and DNA,[12−14] and π-conjugated polymers.[15−19] The isolation of a *specific* chiral (n,m) SWNT from a mixture is dependent on the tube's selective interaction with the dispersing reagents, although the molecular interaction mechanism is poorly understood. Separation based on tube diameters also offers an attractive strategy, as single-chirality separation can be achieved by using dextran-based size-exclusion gel.[20]

In the simple model of aromatic $\pi-\pi$ interaction, two benzene rings can be aligned in either the parallel or perpendicular geometry.[21] When an aromatic dispersant interacts with SWNT, the small molecules such as pyrene and flavin are predominantly aligned in parallel to the SWNT surface for strong intermolecular interaction. The parallel $\pi-\pi$ interaction is also a dominant mechanism for π-conjugated polymer/SWNT complexes in the reported studies so far. While the strong intermolecular interaction facilitates SWNT dispersion, the $\pi-\pi$ interaction also makes it difficult to remove the polymer post SWNT sorting. It is thus desirable to search for a SWNT sorting methodology that uses a weaker intermolecular interaction such as van der Waals forces. Poly[(*m*-phenylenevinylene)-*alt*-(*p*-phenylene-vinylene)] (PmPV) **1** represents an interesting π-conjugated polymer, whose backbone exhibits relative flexibility (Mark−Houwink constant $\alpha \approx 0.85-1.0$)[22] and tends to adopt a helical conformation when dispersing SWNTs.[23] The *para*-phenylene units of PmPV 1 can be aligned either parallel or perpendicular to the SWNT surface (Figure 1) as a modeling study suggests. In this study, we demonstrate that the polymer conformation can be tailored to favor the perpendicular alignment of the π-conjugated segments to SWNT surface (see conformation 4), thereby attenuating its $\pi-\pi$ interaction with SWNT. The strategy is based on the synthesis of PmPV **2**, which bears the water-soluble groups to promote the helical conformation in aqueous solution. In sharp contrast to PmPV **1** which is known to be a good dispersing reagent but exhibits little selectivity toward metallic SWNTs,[23] PmPV **2** revealed drastically improved selectivity in sorting the SWNTs on the basis of tube's diameters.

Received: March 19, 2012
Accepted: May 11, 2012
Published: May 21, 2012

   dx.doi.org/10.1021/mz3001308 | *ACS Macro Lett.* 2012, 1, 701−705

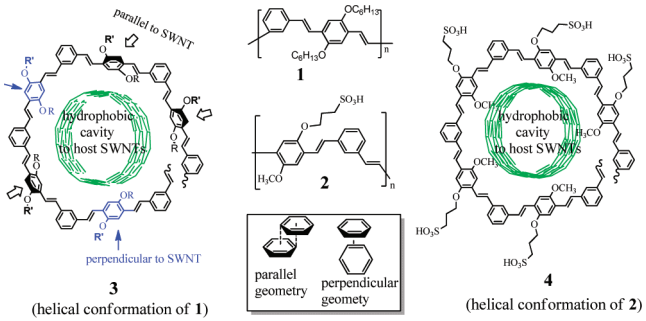

Figure 1. Structure of PmPVs **1** and **2** and proposed respective helical conformations **3** and **4** when wrapping on a (7,5) SWNT. The inset shows the parallel and perpendicular alignment of two benzene rings. The $-OCH_3$ groups in **4** are pointing inward to provide a defined cavity size.

The water-soluble PmPV **2** was synthesized by using Wittig condensation of **5** with isophthaldehyde (Scheme 1). ^{1}H NMR

Scheme 1

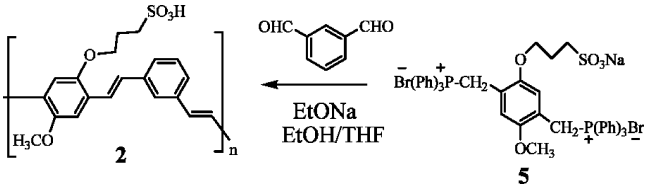

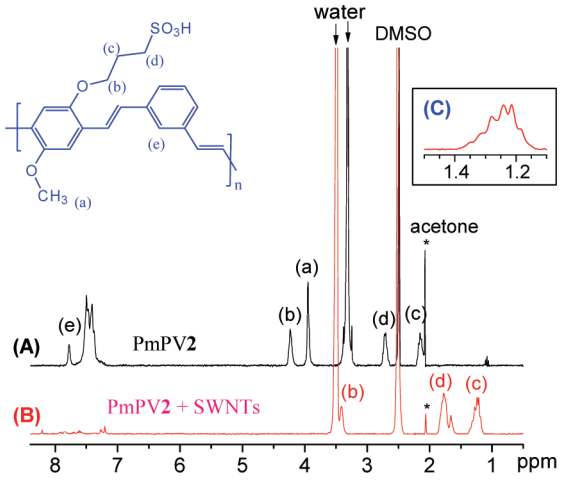

Figure 2. ^{1}H NMR spectra of PmPV **2** (A) and its complex with SWNTs (B) in deuterated DMSO solvent. The protons are labeled by letters a–e. In the bottom spectrum, one drop of D_2O was added to slightly shift the water signal away from the $-OCH_2-$ signal, where the solvent suppression at 3.49 ppm resulted in a lower proton intensity at 3.41 ppm. The starred signal at 2.07 ppm was due to trace acetone in the NMR tube. The inset is the expanded region for proton c of spectrum B, displaying the coupling with adjacent protons.

of PmPV **2** (Figure 2) revealed that the polymer had a regular structure as proposed. The minor aromatic singlet at 7.75 ppm was attributed to H_e, while the remaining aromatic and vinyl signals occurred as a broad multiple peaks at about 7.45 ppm. The protons of $-CH_2O-$ (at 4.24 ppm) and $-OCH_3$ (at 3.94 ppm) each occurred as a broad single peak, indicating that the vinylene bonds were mainly in the *trans*-configuration.[22] By using the end group $-CHO$ detected at ~10 ppm (see Supporting Information (SI) Figure S2), the number average molecular weight was estimated to be ~5000, which corresponds to $n \approx 13$.

The SWNTs were then dispersed by using PmPV solution in deionized water. In a typical dispersion procedure,[23] 3 mg of the SWNTs sample and 20 mL of PmPV in deionized water solution (concn = 10 mg/mL) was mixed, and the mixture was sonicated at 0 °C for two hours. The supernatant solution was then separated from the sediment by centrifugation at 7000 g.

To gain the insight information about the polymer wrapping, the supernatant solution of SWNT/PmPV was examined by ^{1}H NMR, after removal of excess SWNTs and catalysts by further centrifugation at 18 000 g. The resulting sample solution then stayed still for several days to allow establishing equilibrium prior to spectral acquisition. Upon forming a complex with SWNT, the methylene protons H_c and H_d of **2** were shifted upfield by about 1 ppm (Figure 2, bottom spectrum). The methylene signal H_b was buried under the water peak, and the addition of a drop D_2O to the NMR sample caused slight shift of water peak to make the H_b signal visible. The observed upfield shift from protons H_b–H_d was attributed to chain assembly arising from polymer/SWNT interaction, as the free acetone signal at 2.07 ppm was not changed in the presence of SWNTs. The signal of $-OCH_3$, however, was not detected. The signals of vinyl and phenyl protons were dramatically decreased, indicating intimate chain interactions with the SWNT surface. The aromatic protons that are closely associated with SWNTs are known to become undetectable,[24] due to the presence of paramagnetic particle in the SWNT sample. The disappearance of $-OCH_3$ signals, but not H_b ($-OCH_2-$), suggested that the former had a closer interaction with the guest SWNT than the latter, in agreement with the proposed helical wrapping model as shown in **4** (Figure 1). The methylene protons $-CH_2-$ at ~1.24 ppm were detected as an overlapping of two sets of the pentet signal (Figure 2c), since the two methylene protons were differentiated in the assembled environment.

Raman spectra of SWNTs/PmPV revealed that polymer **2** had quite a high selectivity in dispersing (7,5) SWNTs (Figure 3a), in sharp contrast to PmPV **1**.[23] The G-band measured with red excitation wavelength (λ = 647 nm) became relatively narrower for SWNTs/PmPV **2** (see SI, Figure S1a), in agreement with the enrichment of semiconducting SWNT. Raman spectra measured with green laser (λ = 514 nm) showed that the metallic (9,3) SWNT was also selected by the polymer (Figure 3b). Plotting the Raman intensity changes for each SWNT clearly revealed that the polymer selectively enriched the SWNT of smaller diameter (d < 0.9 nm, Figure 3c). The Raman RBM peaks from polymer/SWNTs are shifted to higher frequencies by 5–10 cm^{-1} (SI, Table 1), indicating that SWNTs becomes stiffer[25] after polymer wrapping.

The selectivity was further observed from 2D fluorescence spectra (Figure 4). The signals from SWNTs/PmPV sample were quite weak, as the nanotubes tended to precipitate from the supernatant aqueous solution of polymer/SWNTs. The small diameter (6,5) SWNT was clearly enriched in the SWNTs/PmPV dispersion. While the fluorescence intensity of (7,5) was weaker than that of (7,6) SWNT in the raw sample, the signal of (7,5) was increased to a comparable level in the SWNTs/PmPV complex, in agreement with what was seen in Raman. It appeared that the polymer **2** selectively extracted the SWNTs of smaller diameter, (6,5) and (7,5) SWNTs (d = 0.76

dx.doi.org/10.1021/mz3001308 | ACS Macro Lett. 2012, 1, 701–705

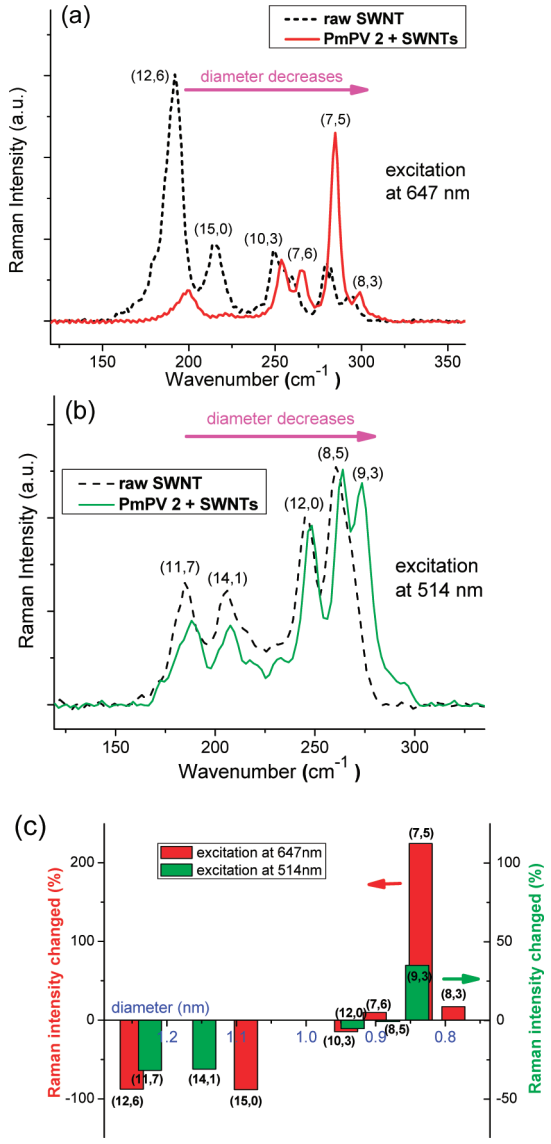

Figure 3. Raman spectra of raw SWNTs in solid in the radial breathing mode (RBM) and SWNTs/PmPV **2** in dispersion, when the samples were excited at 647 nm (a) or at 514 nm (b). Relative SWNT population change plot (c) after dispersion by using PmPV **2**, which is constructed by using a Raman intensity change for each SWNT shown in a and b.

nm and 0.83 nm, respectively).[23,26] The spectra also revealed that those SWNTs with relative large diameters, such as (8,6) and (9,5) (d = 0.97 and 0.98, respectively), were effectively removed.

UV−vis-NIR absorption spectra of the supernatant solution provided consistent evidence that the polymer selectively enriched (7,5), (6,5), and (8,3) SWNTs (Figure S3, SI). Clearly the water-soluble PmPV 2 exhibited notable selectivity toward the SWNTs of small diameters. Interestingly, the sample of SWNT/(PmPV **2**) was depleted of the (12,6) SWNT (see Figure 3a), in contrary to PmPV 1 which slightly enriches (12,6).[23] The drastic difference in the observed selectivity pattern demonstrates the great potential to achieve SWNT separation via control of the polymer conformation.

Different chiral SWNTs present in the raw sample are summarized in Table 1, along with their respective tube diameters.[26] On the basis of the observed selectivity toward

Table 1. Distribution of High-Pressure Carbon Monoxide (HiPco) SWNTs Structure and Diameter in the Studied Sample[a]

SWNTs structures	diameters (nm)	SWNTs structures	diameters (nm)
(6,5) (↑)[c,d]	0.757	(8,6) (↓)[c,d]	0.966
(8,3) (↑)[b,c,d]	0.782	(9,5) (↓)[c,d]	0.976
(9,2) (↑)[c,d]	0.806	(12,1) (↓)[d]	0.995
(7,5) (↑)[b,c,d]	0.829	(8,7) (↓)[c,d]	1.032
(9,3) (↑)[b]	0.847	(10,5) (↓)[d]	1.050
(8,4) (↑)[c,d]	0.840	(15,0) (↓)[b]	1.080
(8,5)	*0.889*	(9,7) (↓)[d]	1.103
(7,6)	*0.895*	(10,6) (↓)[d]	1.111
(9,4) (↓)[d]	0.916	(14,1) (↓)[b]	1.153
(10, 3) (↓)[b,c,d]	0.936	(11,7) (↓)[b]	1.231
(12,0) (↓)[b]	0.940	(12,6) (↓)[b]	1.244

[a]The SWNTs enriched by PmPV 2 are indicated by up arrows (↑), while those decreasing SWNTs are indicated by down arrows (↓). The SWNTs (8,5) and (7,6) are shown in italics, as their selectivities are inconclusive. [b]Supporting evidence for the observed SWNT enrichment: Raman. [c]Supporting evidence for the observed SWNT enrichment: UV-NIR. [d]Supporting evidence for the observed SWNT enrichment: 2D-fluorescence.

(6,5), (7,5), and (9,3) SWNTs, PmPV **2** appeared to have high tendency to host the small tube with relative narrow range of diameters (d = 0.757−0.84 nm). In the meantime, the dispersion of SWNTs/(PmPV 2) was depleted of the SWNTs with larger diameters such as (10,3), (9,5), and

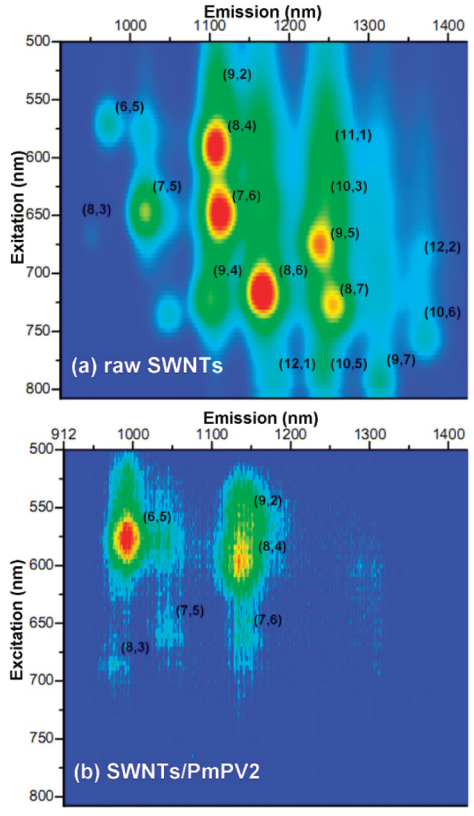

Figure 4. 2D photoluminescence (PL) of SWNT samples (excitation: 500−840 nm; emission: 912−1415 nm). (a) Raw SWNTs were dispersed with the addition of sodium dodecylbenzene sulfonate (SDBS) surfactant (~6% in a mixture of D_2O and H_2O in a ratio of 4:1). (b) SWNTs were dispersed by using PmPV **2** in D_2O.

dx.doi.org/10.1021/mz3001308 | ACS Macro Lett. 2012, 1, 701−705

(12,6) (d > 0.936 nm). The result was in agreement with the enhanced conformation as shown in **4**, as the inner −OMe groups reduce the cavity size that matches the SWNTs of small diameter.

The remarkable difference between **1** and **2**, in terms of SWNT selectivity, could be partially rationalized by considering the substituent impact on the polymer conformational cavity. Since both alkoxy groups in PmPV 1 are hydrophobic, $\pi-\pi$ interaction with SWNT surface becomes an important factor. The *para*-phenylene in **1** thus can be rotated to adopt the parallel interaction with the SWNT surface as shown in the polymer conformation **3** (Figure 1). The assumption is in agreement with the experimental observation that the absorption λ_{max} of **1** in THF was blue-shifted by ∼7 nm when forming the polymer/SWNTs dispersion.[27] As a consequence of the parallel alignment of *para*-phenylene to the SWNT surface, the conformational cavity becomes larger. A wide range of conformational cavity sizes, corresponding to different degrees of *para*-phenylene rotation, permit PmPV **1** to host SWNTs of various diameters. In sharp contrast, PmPV **2** has a strong preference to adopt the conformation **4**, resulting from the strong interaction between water and the hydrophilic substituents. In conformation **4**, the methoxy groups are forced to point inward to confine the conformational cavity, while forming a hydrophobic pocket for SWNTs. The molecular modeling by using HyperChem software showed that the conformational cavity of **4** is slightly larger than 1 nm (Figure S6a, SI). Upon inserting the (7,5) SWNT (d = 0.83 nm) through the polymer conformational cavity, the cavity became larger in the aqueous solvent, partly due to the rotation of the methoxy groups (Figure S6b, SI). All *para*-phenylene units remain to be perpendicular to the nanotube axis, as the conformational cavity size is adjusted to host the SWNTs of small diameters.

An atomic force microscopy (AFM) image of the SWNT/PmPV sample from the supernatant solution revealed that the SWNT was dispersed as a single tube (Figure S4, SI). AFM profilometry (in taping mode) along the lengthwise SWNT direction gave a height profile. From the minimum height of the profile, the diameter of the wrapped nanotube was estimated to be ∼0.9 nm. High resolution TEM further confirmed that the individual nanotubes were dispersed in **2** (Figure S5, SI), without seeing the detail of the polymer wrapping pattern.

The introduction of a water-soluble group on a PmPV chain dramatically improves the chirality selection of SWNT, leading to a sample with a narrow range of diameter (Figure 5). The unsymmetrical substitution pattern, with one substituent on the *para*-phenylene being hydrophilic while the other being hydrophobic, appears to promote the chain folding in aqueous solution for a desirable helical conformation. In addition, the *para*-phenylene rings are preferred to align *perpendicularly* to SWNTs, thereby providing a well-defined hydrophobic cavity to host nanotube of small diameters such as (7,5) SWNT. Interestingly, the selectivity observed from PmPV **2** is in sharp contrast to the structurally similar copolymer, poly{[(*m*-phenylene ethylene)-*alt*-(*p*-phenylene ethylene)]-co-[(*m*-phenylene vinylene)-*alt*-(*p*-phenylene vinylene)] (PPE-PPV), which tends to select SWNTs of large diameters such as (12,6) SWNT.[28] This is because the *para*-phenylene rings in PPE-PPV can easily adopt the *parallel* alignment to SWNT, thereby creating a larger conformational cavity. The distinctive selectivity patterns from PmPV **2**, in comparison with that from PmPV **1** and PPE-PPV, illustrate that the control of polymer conformation can have a profound impact in achieving the desirable SWNT selectivity. The utilization of this strategy, which relies on the cavity size and weak van de Waals interaction, is anticipated to be a useful guide in future molecular design for SWNT separation. On the basis of a weak fluorescence signal (Figure 4b), PmPV **2** appears to have a relatively poor dispersion capability. This could be improved by increasing polymer's water solubility.

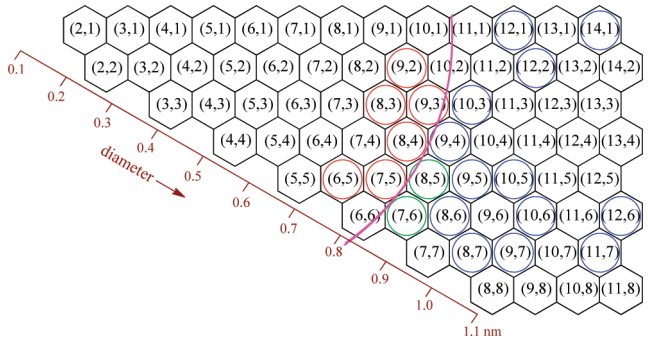

Figure 5. Chirality maps of SWNTs showing that small diameter tubes (red circles) were selected by PmPV **2** wrapping, while the larger tubes (blue circled) were sorted out.

■ ASSOCIATED CONTENT

Supporting Information

Polymer synthesis, SWNT dispersion procedure, Raman spectra in tangential mode (G-band), Raman and fluorescence data, UV−vis-NIR absorption spectrum, and TEM image. This material is available free of charge via the Internet at http://pubs.acs.org.

■ AUTHOR INFORMATION

Corresponding Author

*E-mail: yp5@uakron.edu.

Notes

The authors declare no competing financial interest.

■ ACKNOWLEDGMENTS

This work was supported by AFOSR (Grant FA9550-10-1-0254). A.P.S. acknowledges partial support from the Materials Science and Engineering Division and the SHaRE user Facility, which are sponsored by the Office of Basic Energy Sciences, U.S. Department of Energy. We also thank Professor Mark Foster of University of Akron for assistance in acquiring part of Raman spectra and thank Professor Khalid Lafdi at University of Dayton for assistance in acquiring 2D fluorescence spectra.

■ REFERENCES

(1) Treacy, M. M. J.; Ebbesen, T. W.; Gibson, J. M. *Nature* **1996**, *381*, 678−680.
(2) White, C. T.; Todorov, T. N. *Nature* **1998**, *398*, 240−242.
(3) Ouyang, M.; Huang, J.-L.; Cheung, C. L.; Lieber, C. M. *Science* **2001**, *292*, 702−705.
(4) Ahn, J.-H.; Kim, H.-S.; Lee, K. J.; Jeon, S.; Kang, S. J.; Sun, Y.; Nuzzo, R. G.; Rogers, J. A. *Science* **2006**, *314*, 1754−1757.
(5) Kauffman, D. R.; Star, A. *Chem. Soc. Rev.* **2008**, *37* (6), 1197−1206.
(6) Lemieux, M. C.; Roberts, M.; Barman, S.; Jin, Y. W.; Kim, J. M.; Bao, Z. *Science* **2008**, *321*, 101−103.

(7) Meyyappan, M. *Carbon Nanotubes: Science and Applications*; CRC Press: Boca Raton, FL, 2005.
(8) Joselevich, E.; Dai, H.; Lui, J.; Hata, K.; Windle, A. H. In Carbon Nanotubes; Jorio, A., Dresselhaus, G., Dresselhaus, M. S., Eds.; *Topics in Applied Physics*, Vol. *111*; Springer: Berlin, 2008; pp 101−104.
(9) Komatsu, N.; Wang, F. *Materials* **2010**, *3*, 3818−3844.
(10) Wang, W.; Fernando, K. A. S.; Lin, Y.; Meziani, M. J.; Veca, L. M.; Cao, L.; Zhang, P.; Kimani, M. M.; Sun, Y. P. *J. Am. Chem. Soc.* **2008**, *130* (4), 1415−1419.
(11) Ju, S. Y.; Doll, J.; Sharma, I.; Papadimitrakopoulos, F. *Nat. Nanotechnol.* **2008**, *3*, 356−362.
(12) Zheng, M.; Jagota, A.; Strano, M. S.; Santos, A. P.; Barone, P.; Chou, S. G.; Diner, B. A.; Dresselhaus, M. S.; Mclean, R. S.; Onoa, G. B.; Samsonidze, G. G.; Semke, E. D.; Usrey, M.; Walls, D. J. *Science* **2003**, *302* (5650), 1545−1548.
(13) Tu, X.; Manohar, S.; Jagota, A.; Zheng, M. *Nature* **2009**, *460*, 250−253.
(14) Tu, X.; Hight Walker, A. R.; Khripin, C. Y.; Zheng, M. *J. Am. Chem. Soc.* **2011**, *133* (33), 12998−13001.
(15) Nish, A.; Hwang, J.-Y.; Doig, J.; Nicholas, R. J. *Nat. Nanotechnol.* **2007**, *2*, 640−646.
(16) Hwang, J. Y.; Nish, A.; Doig, J.; Douven, S.; Chen, C. W.; Chen, L. C.; Nicholas, R. J. *J. Am. Chem. Soc.* **2008**, *130* (11), 3543−3553.
(17) Chen, F.; Wang, B.; Chen, Y.; Li, L. J. *Nano Lett.* **2007**, *7* (10), 3013−3017.
(18) Ozawa, H.; Fujigaya, T.; Niidome, Y.; Hotta, N.; Fujiki, M.; Nakashima, N. *J. Am. Chem. Soc.* **2011**, *133*, 2651−2657.
(19) Ozawa, H.; Ide, N.; Fujigaya, T.; Niidome, Y.; Nakashima, N. *Chem. Lett.* **2011**, *40* (3), 239−241.
(20) Liu, H.; Nishide, D.; Tanaka, T.; Kataura, H. *Nature Commun.* **2011**, *2*, 309.
(21) Anslyn, E. V.; Dougherty, D. A. *Modern Physical Organic Chemistry*; University Science Books: Sausalito, CA, 2006; pp 184−185.
(22) Pang, Y.; Li, J.; Hu, B.; Karasz, F. E. *Macromolecules* **1999**, *32*, 3946−3950.
(23) Yi, W.; Malkovskiy, A.; Chu, Q.; Sokolov, A. P.; Colon, M. L.; Meador, M.; Pang, Y. *J. Phys. Chem. B* **2008**, *112* (39), 12263−12269.
(24) Nelson, D. J.; Nagarajan, P. S.; Brammer, C. N.; Perumal, P. T. *J. Phys. Chem. C* **2010**, *114* (22), 10140−10147.
(25) Gotovac, S.; Honda, H.; Hattori, Y.; Takahashi, K.; Kanoh, H.; Kaneko, K. *Nano Lett.* **2007**, *7*, 583−587.
(26) Weisman, R. B.; Bachilo, S. M. *Nano Lett.* **2003**, *3* (9), 1235−1238.
(27) Yi, W.; Malkovskiy, A.; Xu, Y.; Wang, X.; Sokolov, A. P.; Lebron-Colon, M.; Meador, M. A.; Pang, Y. *Polymer* **2010**, *51*, 475−481.
(28) Chen, Y.; Malkovskiy, A.; Wang, X.-Q.; Lebron-Colon, M.; Sokolov, A. P.; Perry, K.; More, K.; Pang, Y. *ACS Macro Lett.* **2012**, *1*, 246−251.